www.elsevier.nl/locate/jorganchem

Journal of Organometallic Chemistry 598 (2000) 87–102

Platinum(II) and palladium(II) compounds derived from $[(\eta^5\text{-}C_5H_5)Fe\{(\eta^5\text{-}C_5H_4)\text{–}CH{=}N\text{–}CH_2\text{–}CH_2\text{–}OH\}]$

Concepción López [a,*], Amparo Caubet [a], Xavier Solans [b], Mercè Font-Bardía [b]

[a] *Departament de Química Inorgànica, Facultat de Química, Universitat de Barcelona, Martí Franquès 1-11, E-08028 Barcelona, Spain*
[b] *Departament de Cristallografía, Mineralogia i Dipòsits Minerals, Facultat de Geologia, Martí Franquès s/n, E-08028 Barcelona, Spain*

Received 17 September 1999; received in revised form 29 October 1999

Abstract

The reactions of the novel ferrocenyl ligand: $[(\eta^5\text{-}C_5H_5)Fe\{(\eta^5\text{-}C_5H_4)\text{–}CH{=}N\text{–}CH_2\text{–}CH_2\text{–}OH\}]$ (**1**) with platinum(II) and palladium(II) salts are described. These reactions have allowed us to isolate and characterize the coordination complexes: $[Pt\{[(\eta^5\text{-}C_5H_4)\text{–}CH{=}N\text{–}CH_2\text{–}CH_2\text{–}OH]Fe(\eta^5\text{-}C_5H_5)\}Cl_2(dmso)]$ (**2**), $[Pd\{[(\eta^5\text{-}C_5H_4)\text{–}CH{=}N\text{–}CH_2\text{–}CH_2\text{–}OH]Fe(\eta^5\text{-}C_5H_5)\}_2Cl_2]$ (**3**) and the cyclopalladated derivative: $[Pd\{[(\eta^5\text{-}C_5H_3)\text{–}CH{=}N\text{–}CH_2\text{–}CH_2\text{–}OH]Fe(\eta^5\text{-}C_5H_5)\}(\mu\text{-}Cl)]_2$ (**4**). Compound **4** reacts with deuterated pyridine, triphenylphosphine or 1,2-bis(diphenylphosphino)ethane giving: $[Pd\{[(\eta^5\text{-}C_5H_3)\text{–}CH{=}N\text{–}CH_2\text{–}CH_2\text{–}OH]Fe(\eta^5\text{-}C_5H_5)\}Cl(L)]$ ($L = \text{py-}d_5$ (**5**) or PPh_3 (**6**)) and $[Pd\{[(\eta^5\text{-}C_5H_3)\text{–}CH{=}N\text{–}CH_2\text{–}CH_2\text{–}OH]Fe(\eta^5\text{-}C_5H_5)\}(dppe)]Cl$ (**7**), which contain a five-membered metallacycle with a $\sigma(Pd\text{–}C_{sp^2,ferrocene})$ bond. The reactions of **4** with *tert*-butylisonitrile or the alkynes: $R\text{–}C{\equiv}C\text{–}R$ (with R = Et, Ph or CO_2Me) are also described and produced: $[Pd\{[(\eta^5\text{-}C_5H_3)\text{–}CH{=}N\text{–}CH_2\text{–}CH_2\text{–}OH]Fe(\eta^5\text{-}C_5H_5)\}Cl(CNCMe_3)]$ (**8**) and the nine-membered palladacycles of general formula: $[Pd\{[(R\text{–}C{=}C\text{–}R)_2(\eta^5\text{-}C_5H_3)\text{–}CH{=}N\text{–}CH_2\text{–}CH_2\text{–}OH]Fe(\eta^5\text{-}C_5H_5)\}Cl(L)]$ (with R = Et (**9**), Ph (**10**) or CO_2Me (**11**)). All the compounds included in this work were characterized by elemental analyses, infrared and NMR spectroscopy. The X-ray crystal structures of **1**, **6**, **8** and **10** are also reported. © 2000 Elsevier Science S.A. All rights reserved.

Keywords: Platinum; Palladium; Cyclopalladation; Ferrocenyl ligand

---

1. Introduction

One of the areas of organometallic chemistry that has attracted great interest during the last decade is that concerning ferrocene derivatives containing heteroatoms with good electron donating abilities (i.e. nitrogen, oxygen, sulfur, phosphorus, etc.) since the coordination of a metal to these heteroatoms produces polymetallic molecules [1–12]. In compounds of this kind the presence of proximal metals may affect the properties of iron(II). For instance, it has been proven that the proclivity of the iron(II) to oxidize depends on several factors [13–23] including the nature of the transition metal and the mode of coordination of the ferrocenyl unit to it. On these basis we attempted to prepare and characterize the novel ferrocenyl Schiff base: $[(\eta^5\text{-}C_5H_5)Fe\{(\eta^5\text{-}C_5H_4)\text{–}CH{=}N\text{–}CH_2\text{–}CH_2\text{–}OH\}]$ (**1**) (Scheme 1), which contains two heteroatoms (N and O) with good electron donating abilities, and to study its reactivity towards platinum(II) or palladium(II) salts.

These reactions could produce different sorts of complexes depending on the mode of coordination of the ligand to the metal atom. The ligand may act as a neutral monodentate group if it binds exclusively to the nitrogen. However, if the deprotonation of the terminal –OH group and/or the activation of the $\sigma(C_{sp^2,ferrocene}\text{–}H)$ bond in the *ortho* site occur, the ligand can also behave as a monoanionic mono-, bi- or terdentate group. In this paper we report the syntheses and characterization of a wide variety of M(II) complexes (M = Pt or Pd) in which ligand **1** acts a monodentate N-donor group or as a monoanionic $(C,N)^-$ bidentate ligand, forming five-membered cyclopalladated complexes with a $\sigma(Pd\text{–}C_{sp^2,ferrocene})$ bond. The reactivity of this bond versus *tert*-butylisonitrile or

---

* Corresponding author. Tel.: + 34-93-402-1274; fax: + 34-93-490-7725.

E-mail address: clopez@kripto.qui.ub.es (C. López)

0022-328X/00/$ - see front matter © 2000 Elsevier Science S.A. All rights reserved.
PII: S0022-328X(99)00682-8

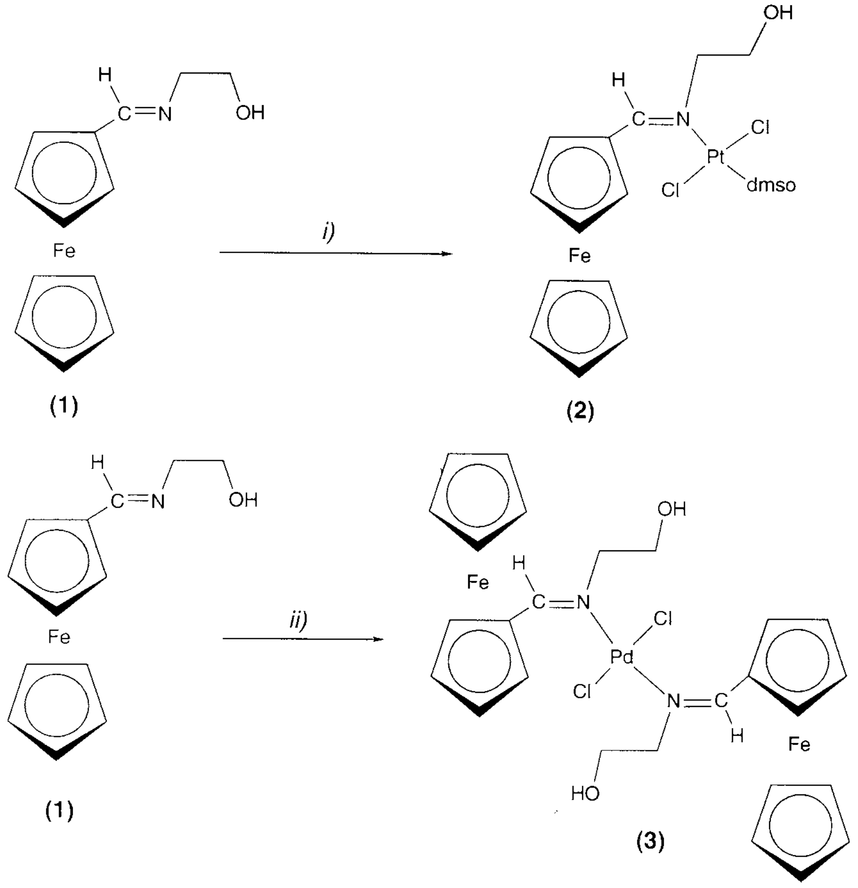

Scheme 1. (i) *cis*-[$PtCl_2(dmso)_2$] in refluxing methanol. (ii) $Na_2[PdCl_4]$ in methanol at room temperature.

the alkynes R–C≡C–R (with R = Et, Ph and CO_2Me) is also reported.

2. Results and discussion

2.1. The ligand

Compound [(η^5-C_5H_5)Fe{(η^5-C_5H_4)–CH=N–CH_2–CH_2–OH}] (**1**) was prepared according to the general procedure described for most ferrocenylketimines [24,25]. This method consists of the reaction of equimolar amounts of ferrocenecarboxaldehyde and the corresponding amine in refluxing benzene, using a Dean–Stark apparatus to remove the benzene–water azeotrope formed during the process, followed by concentration to dryness of the resulting solution. When 2-aminoethanol was used as starting material, this process yielded bright-red needles of ligand **1**.

The ligand was characterized by elemental analyses, infrared and NMR spectroscopy. The elemental analyses were consistent with those expected for the proposed formula (see Section 3). The infrared spectrum showed a sharp, intense band in the range 1620–1640 cm^{-1}, which is assigned to the stretching of the > C=N– group. Despite the fact that ligand **1** could adopt two different forms (*E*- or *Z*-), its ^1H- and $^{13}C\{^1H\}$-NMR (Tables 1 and 2) spectra, which agreed with those reported for related ferrocenyl Schiff bases [24–27], revealed that only one isomer (*E*-form) was present in solution.

Compound [(η^5-C_5H_5)Fe{(η^5-C_5H_4)–CH=N–CH_2–CH_2–OH}] (**1**) has also been characterized by X-ray diffraction. The molecular structure of this compound together with the atom labeling scheme is shown in Fig. 1, and a selection of bond lengths and angles is presented in Table 3.

The structure consists of discrete molecules of [(η^5-C_5H_5)Fe{(η^5-C_5H_4)–CH=N–CH_2–CH_2–OH}] (**1**) separated by van der Waals contacts. The > C=N– bond length (1.25(2) Å) is similar to those reported for related ferrocenyl Schiff bases [26,27] and the ferrocenyl and the CH_2–CH_2OH groups are in a *trans* arrangement as reflected in the torsion angle defined by the set of atoms: C(10), C(11), N and C(12) (− 173.8°), thus indicating that the ligand has the *E*-form. The functional group > C=N– forms an angle of 11.16° with the substituted pentagonal ring of the ferrocenyl fragment.

Bond lengths and angles in the ferrocenyl fragment are consistent with those reported for other ferrocene

Table 1
^{1}H-NMR data (500 MHz, in ppm) for the free ligand (**1**) and for the platinum(II) (**2**) and palladium(II) complexes (**3**–**11**) under study [a]

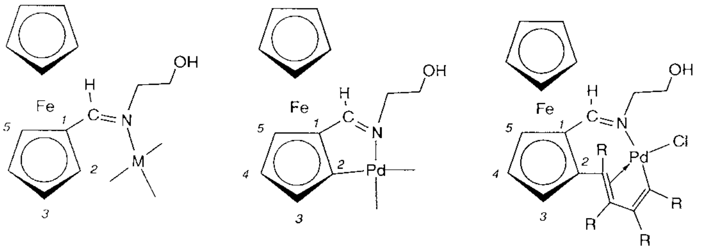

Complex	Ferrocenyl moiety	–CH=N–	>N–CH_2–	–CH_2–	Others
1	4.16, C_5H_5 4.34, H^2, H^5 4.61, H^3, H^4	8.13, s	3.83, t	3.56, t	4.18, t, –OH [b]
2	4.36, C_5H_5 5.64, H^2, H^5 4.73, H^3, H^4	8.15, s [c]	4.30, m	3.85, m	2.91, t, –OH 3.42, s, S–CH_3 [d]
3 [e]	4.35, C_5H_5 5.81, H^2, H^5 4.74, H^3, H^4	7.76, s	4.30, m	3.80, m	3.05, t, –OH
	4.26, C_5H_5 5.61, H^2, H^5 4.59, H^3, H^4	7.76, s	4.41, m	3.60, m	3.10, t, –OH
4 [f]	3.89, C_5H_5 3.80, H^3 3.96, H^4 4.05, H^5	7.72, s	4.10, m [g]	3.60, m [g]	3.49, br, –OH
5 [f,h]	4.34, C_5H_5 3.91, H^3 4.25, H^4 4.46, H^5	8.00, s	4.06, br, m [g]	3.78, br, m [g]	[i]
6 [f]	3.88, C_5H_5 3.33, H^3 4.05, H^4 4.38, H^5	8.14, d [j]	4.17, m 4.05, m	3.90, m 3.75, m	2.75, t, –OH 7.30–8.25, m, Ph
7 [f]	4.04, C_5H_5 3.53, H^3 4.12, H^4 4.60, H^5	8.60, d [j]	3.60, br, m 3.20, br, m	3.30, br, m 3.76, br, m	3.00, br, –OH [k]
8 [f]	4.24, C_5H_5 4.09, H^3 4.28, H^4 4.37, H^5	8.04, s	4.60, br, m 4.22, br, m	3.52, br, m 3.72, br, m	3.40, br, –OH 1.59, s, –CH_3
9 [f]	4.35, C_5H_5 3.94, H^3 4.44, H^4 4.57, H^5	7.92, s	4.20, br, m [g]	3.90, br, m [g]	2.95, t, –OH [l]
10 [f]	4.20, C_5H_5 4.26, H^3 4.35, H^4 4.68, H^5	7.69, s	4.10, br, m	3.28, br, m 3.89, br, m	6.90–7.50, m, Ph [m]
11 [f]	3.71, C_5H_5 4.02, H^3 4.30, H^4 4.61, H^5	7.71, s	4.25, br, m 4.58, br, m	3.28, br, m 3.60, br, m	3.45, t, –OH [n]

[a] Labelling of the atoms refers to the schemes shown above.

[b] Broad and partially overlapped with the signal due to the protons of the C_5H_5 ring.

[c] $^3J(^{195}\text{Pt–H}) = 85$ Hz.

[d] $^3J(^{195}\text{Pt–H}) = 17$ Hz.

[e] See text.

[f] The protons of the –CH_2– moieties are diastereotopic.

[g] Partially overlapped.

[h] In this case the spectrum was recorded in the presence of py-d_5.

[i] Overlapped by the multiplet due to the protons of the –CH_2– group.

[j] Doublet due to phosphorus coupling: $^3J(\text{P–H}) = 8$ Hz (for **6**) and 21 Hz (for **7**).

[k] Two additional multiplets due to the protons of the P–CH_2– groups of the dppe were also observed at 2.06 and 2.60 ppm.

[l] The signals due to the protons of the ethyl groups appeared as four triplets (at 1.60, 1.19, 1.05 and 0.93 ppm, –CH_3 protons) and four multiplets centered at: 2.80, 2.45, 2.37 and 2.20 ppm (–CH_2–).

[m] The signal due to the proton of the –OH group was not observed.

[n] The resonance of the protons of the –OCH_3 fragments appeared as four singlets at 3.99, 3.95, 3.86 and 3.45 ppm.

Table 2
^{13}C-NMR data (in ppm) for the free ligand (**1**) and for the platinum(II) (**2**) and palladium(II) complexes under study [a]

Complex	Ferrocenyl moiety	–CH=N–	>N–CH_2–	–CH_2–	Others
1	69.18, C_5H_5 70.58, C^2, C^5 68.59, C^3, C^4	163.24	63.60	62.25	–
2	70.42, C_5H_5 73.94, C^2, C^5 73.01, C^3, C^4	171.40	67.76	59.96	43.18, S–CH_3 [b]
3 [c]	70.18, C_5H_5 70.22, C_5H_5 72.90 72.08 73.08 72.90	171.56 171.36	67.68 67.31	60.02 59.57	–
4	70.22, C_5H_5 74.99, C^2 68.85, C^3 71.52, C^4 73.08, C^5	171.58	67.30	59.56	–
6 [d]	70.17, C_5H_5 87.02, C^1 102.91, C^2 66.45, C^3 69.15, C^4 68.37, C^5	173.30	63.03	59.43	[e]
7 [f]	70.31, C_5H_5 89.39, C^1 102.91, C^2 68.85, C^3 62.91, C^4 71.60, C^5	178.78	62.91	59.01	[g]
9	70.74, C_5H_5 89.58, C^1 99.69, C^2 70.52, C^3 71.58, C^4 73.41, C^5	165.82	63.61	63.05	12.82 14.30 14.86 17.91 [h] [i]
10	71.90, C_5H_5 86.55, C^1 88.32, C^2 70.30, C^3 73.17, C^4 75.59, C^5	165.93	64.10	62.00	[j]
11	68.97, C_5H_5 74.85, C^2 68.06, C^3 70.98, C^4 72.78, C^5	173.46	65.11	61.47	[k]

[a] Labelling of the atoms refers to the schemes shown at the top of Table 1.

[b] ^2J(Pt–C) = 22.1 Hz.

[c] Two superimposed spectra were detected in this case, due to the inhibition of the rotation around the Pd–N bond (see text).

[d] The signal due to the C^2 carbon appears as a doublet due to phosphorus coupling.

[e] Four additional doublets (centered at ca. 134.74, 131.50, 130.40 and 128.02 ppm) due to the four types of carbon atoms of the phenyl rings of the triphenylphosphine ligand.

[f] The signals due to the carbons: C^1, C^3 and –N–CH_2– appeared as doublets due to phosphorus coupling centered at the values given, and a doublet of doublets was observed for the carbons of the –CH_2–CH_2– fragment of the dppe.

[g] Selected additional data: 30.60 and 27.20, CH_2– of the dppe.

[h] The signals due to the –CH_2– groups of the η^3-butadienyl unit appeared at 35.29, 24.98, 24.42 and 21.89 ppm.

[i] Additional signals at 144.89, 136.88, 177.29 and 108.49 ppm.

[j] Additional signals at: 110.15, 124.64, 126.24, 126.38, 126.80, 127.48, 127.56, 127.82, 127.90, 128.046, 130.95, 134.39, 137.75, 139.72, 140.19, 145.25 and 153.60 ppm.

[k] The signals due to the carbons of the –OCH_3 moieties appeared at: 59.65, 59.43, 58.81 and 52.85 ppm.

derivatives [28]. The two pentagonal rings are planar[1], nearly parallel (tilt angle: 0.59°) and deviate $-3.4°$ from the ideal eclipsed conformation.

2.2. Reactivity of **1** versus platinum(II) and palladium(II) salts

When ligand **1** was treated with *cis*-$[PtCl_2(dmso)_2]$ in refluxing methanol for 3 h, a red solution was obtained. Concentration of this solution on a rotary evaporator to ca. 10 cm^3 produced the precipitation of a red solid, which was identified according to elemental analyses and infrared and ^{1}H-NMR data as $[Pt\{[(\eta^5\text{-}C_5H_4)\text{–}CH{=}N\text{–}CH_2\text{–}CH_2\text{–}OH]Fe(\eta^5\text{-}C_5H_5)\}Cl_2(dmso)]$ (**2**) (Scheme 1).

Quite recently, Wu et al. [29] reported that the reaction of the ferrocenyl ketimine: $[(\eta^5\text{-}C_5H_5)Fe\{(\eta^5\text{-}C_5H_4)\text{–}C(CH_3){=}N\text{–}C_6H_5\}]$ with *cis*-$[PtCl_2(dmso)_2]$ in refluxing methanol produced $[Pt\{[(\eta^5\text{-}C_5H_4)\text{–}C(CH_3){=}N\text{–}C_6H_5]Fe(\eta^5\text{-}C_5H_5)\}Cl_2(dmso)]$ (**2′**). The structural characterization of (**2′**) revealed that the two chlorine groups are in a *trans*-arrangement. On this basis we assumed that compound **2** also corresponds to the *trans*-isomer.

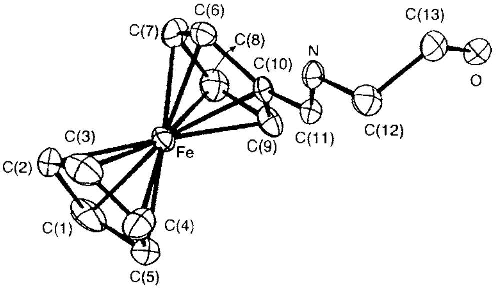

Fig. 1. Molecular structure and atom numbering scheme for the ligand: $[(\eta^5\text{-}C_5H_5)Fe\{(\eta^5\text{-}C_5H_4)\text{–}CH{=}N\text{–}CH_2\text{–}CH_2\text{–}OH\}]$ (**1**).

Table 3
Selected bond lengths (Å) and angles (°) for $[(\eta^5\text{-}C_5H_5)Fe\{(\eta^5\text{-}C_5H_4)\text{–}CH{=}N\text{–}CH_2\text{–}CH_2\text{–}OH\}]$ (**1**) [a]

Bond lengths			
N–C(11)	1.252(5)	N–C(12)	1.467(6)
O–C(13)	1.389(6)	C(10)–C(11)	1.459(6)
C(12)–C(13)	1.496(7)	Fe–C_{ring} [b]	2.017(5)
C–C_{ring} [b]	1.398(21)		
Bond angles			
C(6)–C(10)–C(11)	127.9(4)	C(9)–C(10)–C(11)	123.7(4)
C(10)–C(11)–N	122.9(4)	C(11)–N–C(12)	117.6(4)
N–C(12)–C(13)	109.5(4)	C(12)–C(13)–O	109.2(4)

[a] Estimated S.D. values in parenthesis.

[b] Average values for the ferrocenyl moiety.

The reaction of the ferrocenyl Schiff base **1** with a stoichiometric amount of $Na_2[PdCl_4]$ in methanol at room temperature produced an orange solid. Its characterization data based on elemental analyses and IR and NMR spectroscopic data were consistent with those expected for $[Pd\{[(\eta^5\text{-}C_5H_4)\text{–}CH{=}N\text{–}CH_2\text{–}CH_2\text{–}OH]Fe(\eta^5\text{-}C_5H_5)\}_2Cl_2]$ (**3**) (Scheme 1). This compound was obtained in higher yield when the reaction was performed using a two-fold excess of the imine **1**.

However, when the reaction was carried out in the presence of a stoichiometric amount of $Na(CH_3COO)\cdot 3H_2O$, the di-μ-chloro-bridged cyclopalladated complex: $[Pd\{[(\eta^5\text{-}C_5H_3)\text{–}CH{=}N\text{–}CH_2\text{–}CH_2\text{–}OH]Fe(\eta^5\text{-}C_5H_5)\}(\mu\text{-}Cl)]_2$ (**4**) was obtained (Scheme 2). This compound arises from the activation of a $\sigma(C_{sp^2,ferrocene}\text{–}H)$ bond and contains two five-membered palladacycles. These results are consistent with those reported previously for related ferrocenyl aldimines and ketimines, for which the activation of the $\sigma(Pd\text{–}C_{sp^2,ferrocene})$ required the presence of a base such as $NaCH_3COO$ [24,25,30,31].

Complex **4** undergoes bridge-splitting reactions in the presence of deuterated pyridine (py-d_5) in $CDCl_3$ or triphenylphosphine (PPh_3) in benzene to give the corresponding monomeric derivatives: $[Pd\{[(\eta^5\text{-}C_5H_3)\text{–}CH{=}N\text{–}CH_2\text{–}CH_2\text{–}OH]Fe(\eta^5\text{-}C_5H_5)\}Cl(L)]$, with L = py-$d_5$ (**5**) or PPh_3 (**6**) (Scheme 2), in which the ligand acts as a monoanionic $(C,N)^-$ group.

When 1,2-bis(diphenylphosphino)ethane was added to a CH_2Cl_2 suspension of **4** at room temperature (ca. 20°C), dissolution of the starting material immediately took place. Concentration of the resulting mixture on a rotary evaporator to ca. 5 cm^3 followed by the slow evaporation of the solution at room temperature (ca. 20°C) produced a red microcystalline material. Its characterization data, based on elemental analyses and infrared and NMR {^{1}H, ^{13}C and ^{31}P} spectroscopies were consistent with those expected for: $[Pd\{[(\eta^5\text{-}C_5H_3)\text{–}CH{=}N\text{–}CH_2\text{–}CH_2\text{–}OH]Fe(\eta^5\text{-}C_5H_5)\}(dppe)]Cl$ (**7**) (Scheme 2).

2.3. Study of the reactivity of the $\sigma(Pd\text{–}C_{sp^2,ferrocene})$ bond in $[Pd\{[(\eta^5\text{-}C_5H_3)\text{–}CH{=}N\text{–}CH_2\text{–}CH_2\text{–}OH]Fe(\eta^5\text{-}C_5H_5)\}(\mu\text{-}Cl)]_2$ (4)

Cyclopalladated complexes are particularly relevant due to the high reactivity of the σ(Pd–C) bond, which has provided new methods for the syntheses of organic and organometallic compounds [32–34]. Most of these reactions are based on the insertion of small molecules (mainly alkynes and to a lesser extent, isonitriles, alkenes or CO) into the σ(Pd–C) bond. On this basis, complex **4** appeared to be a good candidate for the study of the reactivity of the $\sigma(Pd\text{–}C_{sp^2,ferrocene})$ bond

---

[1] The least-squares equation of the planes defined by the sets of atoms [C(1)–C(5)] and [C(6)–C(10)] are the following: $(0.6873)XO + (0.6835)YO + (-0.2456)ZO = 2.6326$ and $(0.6859)XO + (0.6813)YO + (-0.2557)ZO = 5.8573$.

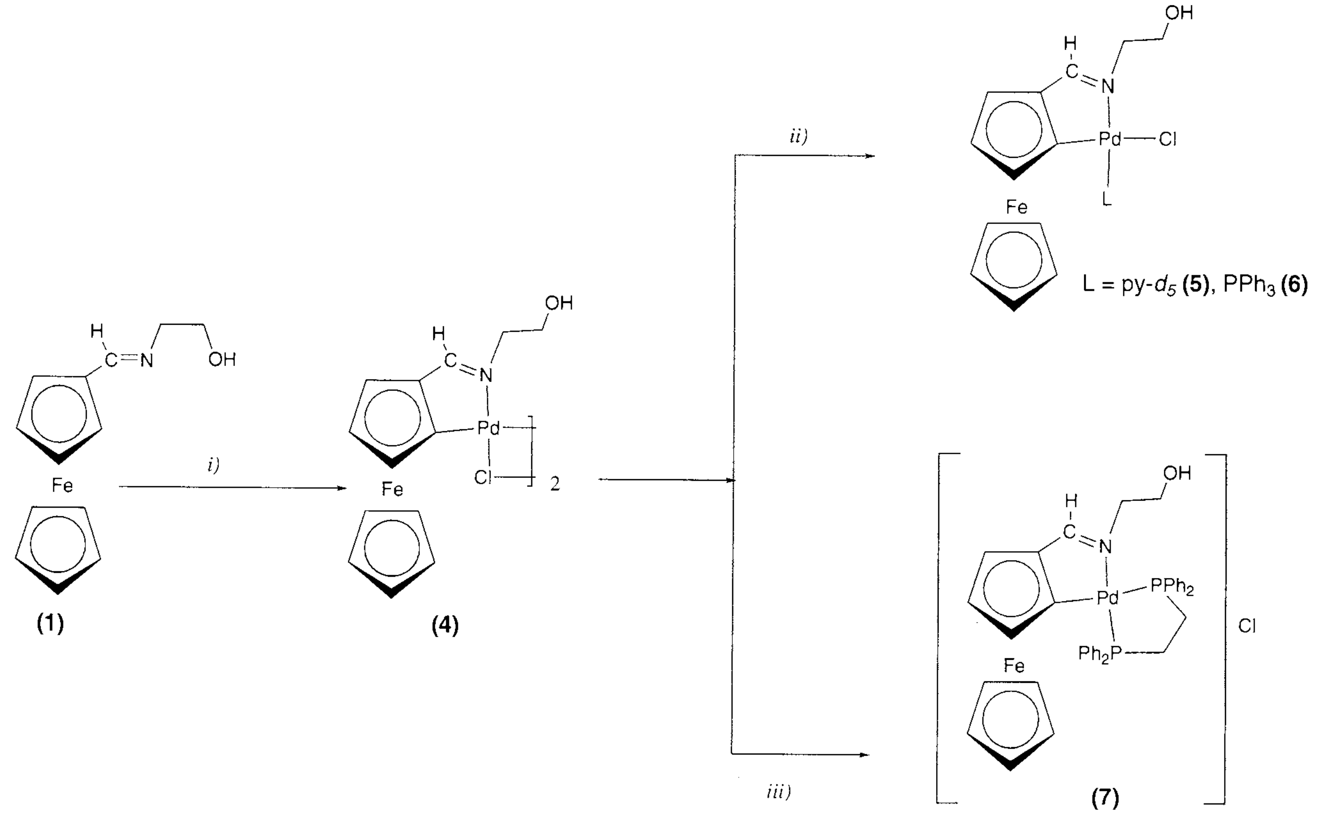

Scheme 2. (i) $Na_2[PdCl_4]$, $Na(CH_3COO)\cdot 3H_2O$ in methanol at room temperature. (ii) L = py-d_5 (in ($CDCl_3$) or PPh_3 in benzene at room temperature. (iii) 1,2-Bis(diphenylphosphino)ethane (dppe) in CH_2Cl_2 at room temperature.

versus *tert*-butylisonitrile or the alkynes R–C≡C–R (with R = Et, Ph or CO_2Me), which differ in the electronic and steric nature of the substituents [35].

In a first attempt to study the reactivity of the cyclopalladated complex **4** versus the *tert*-butylisonitrile, the procedure described by Albinati and co-workers [34] was used. This method consists of the reaction of the di-μ-chloro-bridged cyclopalladated derivative with an excess of the isonitrile and 1,2-bis(diphenylphosphino)ethane in CH_2Cl_2 at room temperature. When the reaction was carried out using compound **4** two products were isolated (Scheme 3(A)). The characterization data of one of them was identical to those obtained for complex **7**, which contains a five-membered metallacycle where the diphosphine acts as a neutral (P,P′) bidentate ligand. Elemental analyses and NMR data of the second component confirmed those expected for: $[Pd\{[(\eta^5\text{-}C_5H_3)\text{–}CH{=}N\text{–}CH_2\text{–}CH_2\text{–}OH]Fe(\eta^5\text{-}C_5H_5)\}Cl(CNC\text{-}Me_3)]$ (**8**). This complex arises from the bridge-splitting reaction and the coordination of the isonitrile to the palladium(II). The X-ray crystal structure of compound **8** (see below) confirms these results. Compound **8** can be obtained in higher yield by treatment of **4** with a two-fold excess of the isonitrile in CH_2Cl_2.

The results obtained in the reaction of **4** with *tert*-butylisonitrile are in contrast with those reported for $[Pd\{5'\text{-}OCH_3\text{–}C_6H_3\text{–}CH{=}N\text{–}C_6H_4\text{-}4\text{-}CH_3\}(\mu\text{-}Cl)]_2$ (**Ia**) which produces the ketimine (**IIa** in Scheme 3(B)) under identical experimental conditions [34]. These findings suggest that compound **4** is less prone to undergo the insertion of *tert*-butylisonitrile than $[Pd\{5'\text{-}OCH_3\text{–}C_6H_3\text{–}CH{=}N\text{–}C_6H_4\text{-}4\text{-}CH_3\}(\mu\text{-}Cl)]_2$ (**Ia**).

In contrast with these results, when complex **4** was treated with the alkynes R–C≡C–R (with R = Et, Ph or CO_2Me) in a 1:4 molar ratio in refluxing chloroform for 1.5 h, the cyclopalladated complexes of general formula: $[Pd\{[(R\text{–}C{=}C\text{–}R)_2(\eta^5\text{ - }C_5H_3)\text{–}CH{=}N\text{–}CH_2\text{–}CH_2\text{–}OH]\text{-}Fe(\eta^5\text{-}C_5H_5)\}Cl]$ (with R = Et (**9**), Ph (**10**) or CO_2Me (**11**)) were isolated (Scheme 4), and no evidence of the formation of any other palladium(II) complex was detected by NMR spectroscopy.

Compounds **9**–**11** arise from the bis(insertion) of the corresponding alkyne into the $\sigma(\text{Pd–C}_{\text{sp}^2\text{,ferrocene}})$ and contain a nine-membered palladacycle. The X-ray crystal structure of $[Pd\{[(Ph\text{–}C{=}C\text{–}Ph)_2(\eta^5\text{-}C_5H_3)\text{–}CH{=}N\text{–}CH_2\text{–}CH_2\text{–}OH]Fe(\eta^5\text{-}C_5H_5)\}Cl]$ (**10**) described below confirms these results.

It is widely accepted that the nature of the final product formed in the reaction of alkynes and cyclopalladated complexes containing $\sigma(\text{Pd–C}_{\text{sp}^2\text{,aryl}})$ bonds depends on a wide variety of factors including: (a) the nature of the substituents (R) of the alkyne; (b) the structure and

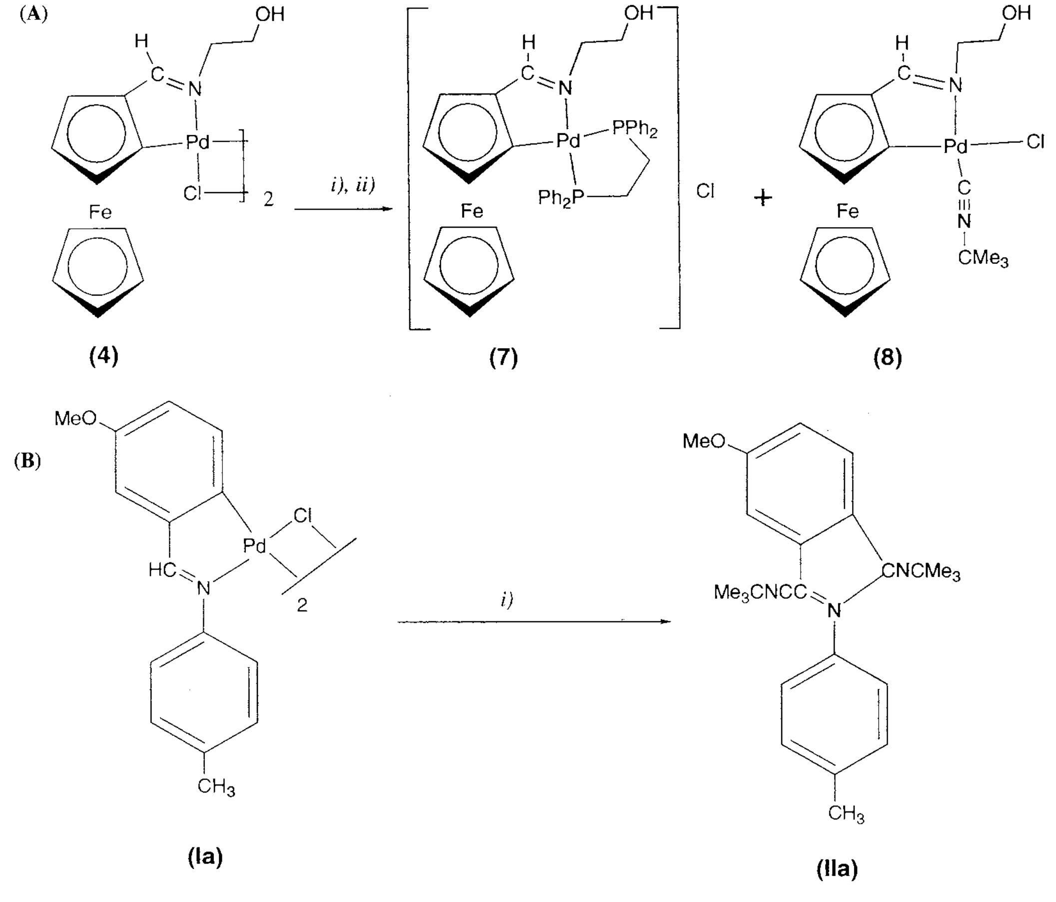

Scheme 3. (i) CNCMe$_3$ and dppe in CH$_2$Cl$_2$ at room temperature. (ii) SiO$_2$, column chromatography, using CHCl$_3$ as eluent.

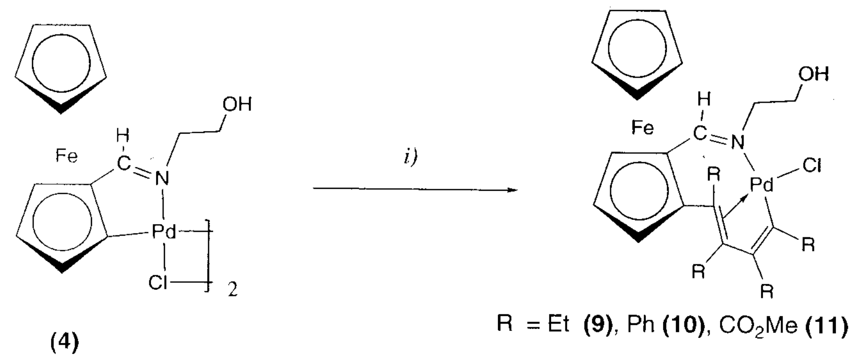

Scheme 4. (i) R–C≡C–R in refluxing CHCl$_3$, 1.5 h, followed by SiO$_2$ column chromatography, using a 100:1 CHCl$_3$–CH$_3$OH mixture as eluant.

nature of the metallated ligand; (c) the stoichiometry; (d) the lability of the Pd–N bond; and (e) the remaining ligands bound to the palladium [32]. In the reactions under study, the nature of the sub stituent of the alkyne was the only variable introduced in all the reactions [35]. It has been postulated that for the insertion of alkynes into the σ(Pd–C$_{sp^2,aryl}$) bond of cyclopalladated complexes containing *N*,*N*-dimethylbenzylamines, the electron-donating or electron-withdrawing nature of the substituents (R) of the alkynes appears to play a crucial role in determining the nature of the final product (a mono(insertion) or a bis(insertion) derivative) [36]. Although the R groups of the three alkynes used in this study have different electronic properties [35], the formation of the bis(insertion) products is strongly favored in all cases.

In addition, it is also interesting to compare the results obtained in the reaction of **4** with the alkyne: MeO$_2$C–C≡C–CO$_2$Me with those reported for the cyclopalladated complexes: [Pd{R–C$_6$H$_3$–CH=N–C$_6$H$_4$-4-CH$_3$}(μ-CH$_3$COO)]$_2$ (**I**) (with R = 5-NO$_2$ (**Ib**), 4-NO$_2$ (**Ic**), 5-Cl (**Id**) or 4-Cl (**Ie**)) (Scheme 5). Addition of an excess of the alkyne to the bridged acetate dimers containing electron-withdrawing R groups (**Ib**–**e**) pro-

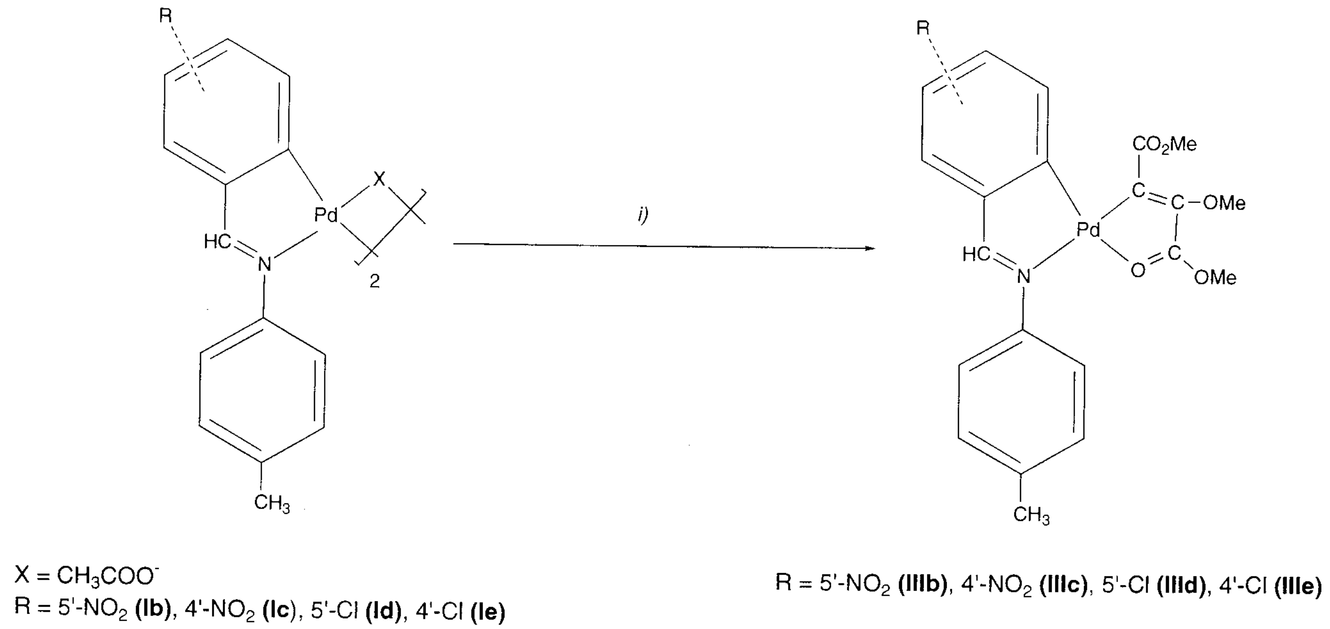

Scheme 5. (i) $MeO_2C–C≡C–CO_2Me$ in methanol, 40°C, 12 h.

duced $[Pd\{R–C_6H_3–CH=N–C_6H_4\text{-}4\text{-}CH_3\}\{OC(OCH_3)–C(OCH_3)=C(COOCH_3)\}]$ (**IIIb**–**e**) in fairly good yields (in the range: 70–90%) [34]. The nature of compounds **III**, which contain a five-membered palladacycle and a six-membered chelate ring, is markedly different from that of **11** in which a nine-membered palladacycle is formed through the bis(insertion) of the $MeO_2C–C≡C–CO_2Me$ into the $\sigma(Pd–C_{sp^2,ferrocene})$ bond. The differences observed in the reactivity of compounds **I** and **4** versus this alkyne may be related to the nature of the metallated carbon ($C_{sp^2,aryl}$ in **I** and $C_{sp^2,ferrocene}$ in **4**), the different lability of the Pd–N bond, or even the remaining ligands bound to the palladium. All these factors may modify the net charge of the metallated carbon. According to the literature, this factor plays a crucial role in the reactions of cyclopalladated complexes with alkynes [36].

2.4. Characterization of the platinum(II) and palladium(II) compounds

Compounds **2**–**6** were characterized by elemental analyses and infrared and NMR spectroscopies. Except for compound **5**, which was prepared and characterized in situ, for the remaining complexes, the elemental analyses (see Section 3) are consistent with the proposed formulae. The most outstanding feature observed in the IR spectra of these complexes is the band due to the stretching of the imine group, which appears in the range: 1560–1640 cm^{-1}. It is noteworthy that in the five-membered cyclopalladated complexes **4**, **6**–**8** this band appears strongly shifted to lower wavenumbers than in the coordination complexes **2**, **3**.

^1H-NMR spectroscopic data for compounds under study are summarized in Table 1. The ^1H-NMR spectrum of **2** showed the typical pattern of monosubstituted ferrocene derivatives: three signals of relative intensities 2:2:5 in the range 5.00–3.50 ppm. In contrast with these results, the spectrum of **3** exhibited higher complexity and some of the signals appeared in duplicate, which suggested the existence of two isomeric species in solution. In an initial attempt to explain the complexity of the ^1H-NMR spectrum, a molecular model of the *trans*-isomer of **3** was constructed. Its manipulations revealed that a coplanar arrangement between the '$PdCl_2$' fragment and the backbone of the imine group is not possible since such an orientation would involve short contacts between one of the chlorines and the *ortho*-hydrogen of the C_5H_4 ring. In order to confirm these facts, the pm3(tm) program included in the SPARTAN package [37] was used. For this arrangement of groups, the estimated $Cl\cdots H_{ortho}$ distance obtained by the program is too small (0.66 Å). A nearly orthogonal orientation of the '$PdCl_2$' fragment and the imine groups significantly reduces the steric hindrance. Consequently, this steric repulsion precludes free rotation around the Pd–N bond. Thus, it would seem that the complexity of the ^1H-NMR spectrum might be due to the presence of rotameric species (Fig. 2(A and B)), which differ in the relative arrangement of the '$Fe(\eta^5\text{-}C_5H_5)$' moieties in each one of the ligands.

The $^{13}C\{^1H\}$-NMR data (see below) are consistent with this hypothesis. However, it should be noted that for compounds: *trans*-$[Pd(R^1C(R^2)=N–NR^3R^4)Cl_2]$ (where R^1 = H, Me, Et; R^2 = Me, Et or ^{i}Pr, R^3 = Me or Et and R^4 = Me} [38] and *trans*-$[Pd\{(\eta^5\text{-}C_5H_5)Fe\{(\eta^5\text{-}$

C_5H_4)–CH=N–NMe_2}Cl_2] (**3′**) [39] the complexity of the NMR spectra was also interpreted in terms of the presence of rotameric species in solution. As well as this, the X-ray crystal structure of (**3′**) confirmed a nearly orthogonal arrangement of the imine fragments versus the '$PdCl_2$' moiety [39].

The ^1H-NMR spectra of the cyclopalladated derivatives **4**–**11** showed the typical pattern of 1,2-disubstituted ferrocene complexes, i.e. four signals of relative intensities 1:1:1:5 in the range 3.50–4.80 ppm.

^{13}C-NMR spectroscopic data are presented in Table 2; the signals were assigned on the basis of 2D-heteronuclear {^1H–^{13}C}-NMR experiments. The $^{31}P\{^1H\}$-NMR spectrum of **6** showed a singlet at 37.40 ppm. The position of this signal is consistent with a *trans* arrangement between the PPh_3 ligand and the imine nitrogen [24,26,31,40–42]. For compound **7**, which contains two phosphorus atoms in different environments, the $^{31}P\{^1H\}$-NMR spectra showed two doublets centered at 48.04 and 62.38 ppm in close accord with the results obtained for [Pd{[(η^5-C_5H_3)–CH=N–R]Fe{(η^5-C_5H_5)}(dppe)]Cl, with R = phenyl or benzyl groups [24].

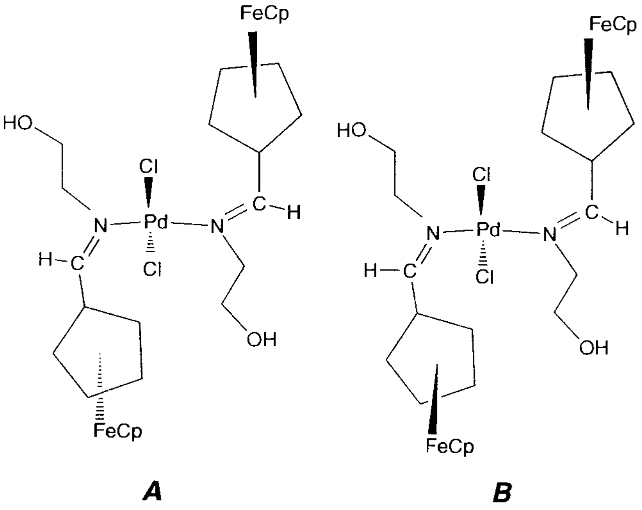

Fig. 2. Schematic view of the two isomers A and B of **3** present in solution. In the figure the dashed lines indicate that they are in a lower plane. The main difference between the two isomer is found in the relative orientation of the 'Fe(η^5-C_5H_5)' moieties in each one of the ligands. In A the two 'Fe(η^5-C_5H_5)' fragments are on the same side of one of the chlorines; while in B each one of the 'Fe(η^5-C_5H_5)' moieties is facing a different chlorine, and in this case the whole molecule is centrosymmetric.

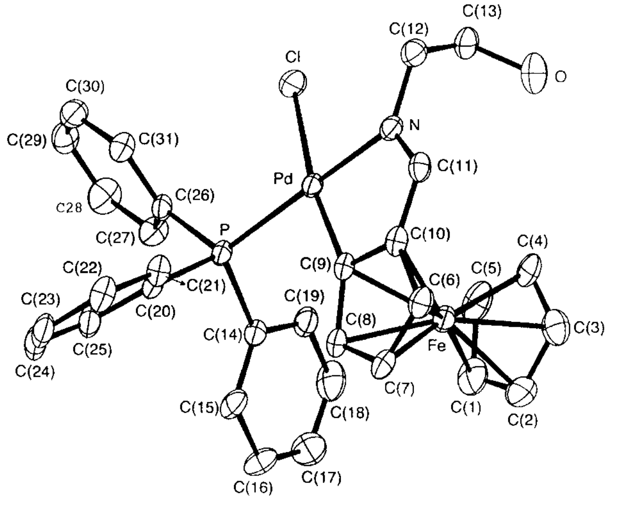

Fig. 3. Molecular structure and atom numbering scheme for: [Pd{[(η^5-C_5H_3)–CH=N–CH_2–CH_2–OH]Fe(η^5-C_5H_5)}Cl(PPh_3)] (**6**).

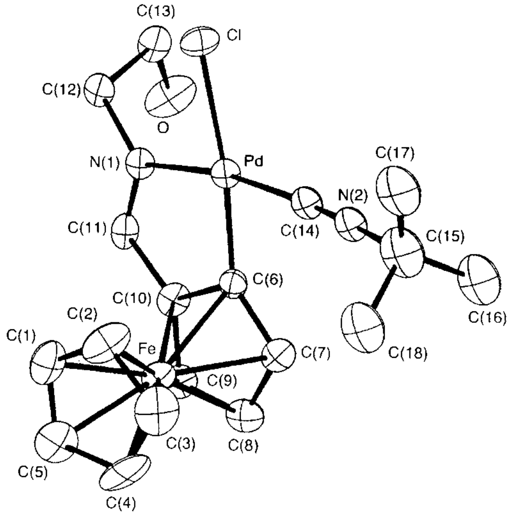

Fig. 4. Molecular structure and atom numbering scheme for: [Pd{[(η^5 - C_5H_3)–CH=N–CH_2–CH_2–OH]Fe(η^5 - C_5H_5)}Cl(CNCMe$_3$)] (**8**)

Compound **2** was also characterized by $^{195}Pt\{^1H\}$-NMR spectroscopy. The spectrum showed a complex signal at − 3025 ppm. The position of the signal is consistent with the ^{195}Pt chemical shifts reported for *cis*-[$PtCl_2(NH_3)$(dmso)] (δ = − 3046 ppm [43]), [Pt_2{Fe[(η^5-C_5H_4)–CH_2–N(CH_3)$_2$]$_2$}Cl_4(dmso)$_2$] (δ = − 3006 ppm [44]) or related platinum(II) complexes containing a ($NSCl_2$) environment around the platinum [43,45,46]. The complexity of the signal could be due to the coupling between the platinum(II) and the protons of the N–CH_2– group and/or of the methyl groups of the coordinated dmso ligand.

Compounds [Pd{[(η^5-C_5H_3)–CH=N–CH_2–CH_2–OH]-Fe(η^5-C_5H_5)}Cl(PPh_3)] (**6**) and [Pd{[(η^5-C_5H_3)–CH=N–CH_2–CH_2–OH]Fe(η^5-C_5H_5)}Cl(CNCMe$_3$)] (**8**) were also characterized by X-ray diffraction. The molecular structure of these complexes together with the atom labeling schemes are shown in Figs. 3 and 4, respectively. A selection of bond lengths and angles is presented in Tables 4 and 5.

These structures consist of discrete molecules of [Pd{[(η^5-C_5H_3)–CH=N–CH_2–CH_2–OH]Fe(η^5-C_5H_5)}-Cl(PPh_3)] (in **6**) or [Pd{[(η^5-C_5H_3)–CH=N–CH_2–CH_2–

OH]Fe(η^5-C_5H_5)}Cl(CNCMe$_3$)] (in **8**) separated by van der Waals contacts. The palladium is bound to the chlorine, the imine nitrogen, the *ortho*-carbon of the ferrocenyl fragment (C(9) in **6** or C(6) in **8**) and the phosphorus of the PPh_3 ligand in **6** or the terminal carbon atom of the isonitrile (C(14)) in **8** in a slightly distorted square-planar environment[2]).

In the two cases, the metallacycles are practically planar[3] and contain the > C=N– functional group, thus confirming the *endo*-type structure predicted by ^{1}H- and ^{13}C-NMR spectroscopies. The palladacycles are practically co-planar with the C_5H_3 ring of the ferrocenyl moiety (the dihedral angle formed by the normals to their main planes is 4.71° in **6** and 3.57° in **8**). The > C=N– bond distance (1.278(5) Å in **6** or 1.272(6) Å in **8**) is similar to the distances found in related five-membered palladacycles with σ(Pd–$C_{sp^2,ferrocene}$) bonds and is slightly greater, if significant, than that of the free ligand (1.252(5) Å). The ferrocenyl- and the CH_2–CH_2OH groups are in a *trans*-arrangement, thus indicating that the ligand retains the *E*-form during the reaction.

In compound **8** the isonitrile group is bound to the palladium through the terminal carbon (C(14)) and the fragments: Pd–C(14)–C(15) and C(14)–N(2)–C(15) are practically linear (bond angles 176.2(5) and 174.4(6)°, respectively). The torsion angle Pd–C(14)–N(2)–C(15) is − 49.82°.

Table 4
Selected bond lengths (Å) and angles (°) for [Pd{[(η^5-C_5H_3)–CH=N–CH_2–CH_2–OH]Fe(η^5-C_5H_5)}Cl(PPh_3)] (**6**) [a]

Bond lengths			
Pd–P	2.240(2)	Pd–Cl	2.375(2)
Pd–N	2.135(4)	Pd–C(9)	1.998(4)
C(9)–C(10)	1.447(6)	C(10)–C(11)	1.424(6)
N–C(11)	1.278(5)	N–C(12)	1.457(6)
C(12)–C(13)	1.513(7)	C(13)–O	1.395(6)
Fe–C_{ring} [b]	2.043(11)	C–C_{ring} [b]	1.413(20)
Bond angles			
N–Pd–C(9)	80.9(2)	P–Pd–C(9)	92.21(13)
N–Pd–P	170.24(9)	Cl–Pd–C(9)	171.44(11)
N–Pd–Cl	92.31(11)	P–Pd–Cl	95.14(7)
Pd–N–C(11)	113.1(3)	Pd–N–C(12)	126.8(3)
Pd–C(9)–C(10)	111.0(3)	C(10)–C(11)–N	117.3(4)
C(11)–N–C(12)	120.0(4)	N–C(12)–C(13)	112.5(4)
C(12)–C(13)–O	109.7(4)		

[a] Estimated S.D. values in parenthesis.
[b] Average value for the ferrocenyl moiety.

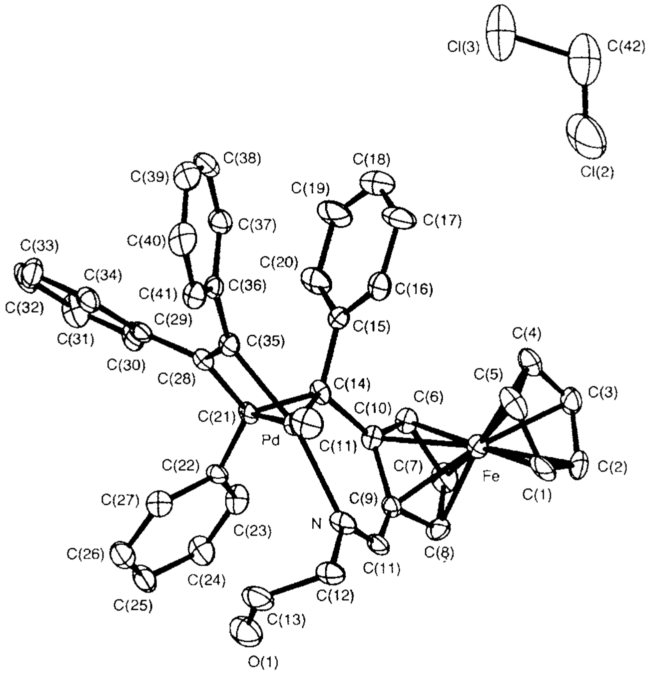

Fig. 5. Molecular structure and atom numbering scheme for: [Pd{[(Ph–C=C–Ph)$_2$(η^5-C_5H_3)–CH=N–CH_2–CH_2–OH]Fe(η^5-C_5H_5)}-Cl] (**10**).

Table 5
Selected bond lengths (Å) and angles (°) for [Pd{[(η^5-C_5H_3)–CH=N–CH_2–CH_2–OH]Fe(η^5-C_5H_5)}Cl(CNCMe$_3$)] (**8**) [a]

Bond lengths			
Pd–C(14)	1.991(5)	Pd–Cl	2.394(2)
Pd–N	2.080(4)	Pd–C(6)	1.951(5)
C(9)–C(10)	1.414(7)	C(10)–C(11)	1.423(6)
N–C(11)	1.272(6)	N–C(12)	1.451(5)
C(12)–C(13)	1.513(7)	C(13)–O	1.411(7)
C(14)–N(2)	1.131(6)	N(2)–C(15)	1.472(9)
C(15)–C(16)	1.472(12)	C(15)–C(17)	1.392(12)
C(15)–C(18)	1.453(12)	Fe–C_{ring} [b]	2.02(2)
C–C_{ring} [b]	1.39(2)		
Bond angles			
N–Pd–C(6)	81.1(2)	C(14)–Pd–C(6)	92.21(13)
N–Pd–C(14)	169.6(2)	Cl–Pd–C(9)	171.44(11)
N–Pd–Cl	92.31(11)	P–Pd–Cl	95.14(7)
Pd–N–C(11)	113.1(3)	Pd–N–C(12)	126.8(3)

[a] Estimated S.D. values in parenthesis.
[b] Average value for the ferrocenyl moiety.

---

[2] For **6**: the least-squares equation of the plane defined by the atoms Pd, Cl, P, N and C(9) is: (− 0.1453)XO + (0.8876)YO + (− 0.4371)ZO = − 3.3167. The deviations from the mean plane are: Pd, + 0.014; P, − 0.100; Cl, + 0.086; and N, − 0.012 Å. For **8**: the least-squares equation of the plane defined by the atoms Pd, Cl, N(1), C(8) and C(14) is: (− 0.6051)XO + (0.7082)YO + (− 0.3638)ZO = 10.1058. The deviations from the mean plane are: Pd, + 0.0297; Cl, − 0.0354; N(1), + 0.0271; C(8), − 0.0483; and C(14), 0.0269 Å.

[3] For **6**: The least-squares equation of the plane defined by the atoms Pd, N, C(9), C(10) and C(11) is: (− 0.1045)XO + (0.9248)YO + (− 0.3658)ZO = − 2.3622. The deviations from the mean plane are: Pd, + 0.0172; N, − 0.0.0161; C(9), + 0.0231; C(10), − 0.0180; and C(10), − 0.0040 Å. For **8**: the least-squares equation of the plane defined by the atoms Pd, N(1), C(8), C(10) and C(11) is: (− 0.6634)XO + (0.6894)YO + (0.2905)ZO = 9.4569. The deviations from the mean plane are: Pd, − 0.0268; N(1), 0.0729; C(8), + 0.0303; C(10), − 0.0345; and C(14), − 0.0419 Å.

Bond lengths and angles in the ferrocenyl fragment are very similar to those reported for other ferrocene derivatives [28]. The two pentagonal rings are planar[4]), nearly parallel (tilt angles: 1.03 and 4.27° for **6** and **8**, respectively) and they deviate from the ideal eclipsed conformation by − 3.74° in **6** and by 1.75° in **8**. The long distance between the Fe(II) and the Pd(II) ions (3.5635(3) Å in **6** or 3.5020(3) Å in **8**) suggests that there is no direct interaction.

The molecular structure of compound **10** and the atom labeling scheme are shown in Fig. 5, and a selection of bond lengths and angles is presented in Table 6.

The structure consists of discrete molecules of $[Pd\{[(Ph{-}C{=}C{-}Ph)_2(\eta^5{-}C_5H_3){-}CH{=}N{-}CH_2{-}CH_2{-}OH]{-}Fe(\eta^5{-}C_5H_5)\}Cl]$ separated by van der Waals contacts and also contains a molecule of CH_2Cl_2 as solvate. The palladium is tetracoordinated bound to a chlorine (Cl(1)), the nitrogen, C(35) and the middle point of the segment defined by the atoms C(14) and C(21) (hereafter referred to as χ) in a distorted square planar environment. The deviations from the mean plane[5]) are as follows: Cl(1), 0.1534; N, − 0.1528; C(35), − 0.2036 and χ, 0.2031 Å. The Pd–N, Pd–Cl(1) and Pd–C(35) bond lengths are similar to those found in five-membered cyclopalladated complexes [14,21,24–28,40,41]. The palladium is symmetrically bound to the carbons C(14) and C(21) (Pd–C(14): 2.085(4) Å and Pd–C(21): 2.085(4) Å) and the angle C(14)–Pd–C(21) is 39.6(2)°. The C(14)–C(21) double bond forms a dihedral angle of 70.97° with the coordination plane of the complex. The C(14)–C(21) bond length is clearly longer (1.427(6) Å) than the C(28)–C(35) double bond (1.294(5) Å), and this difference can be attributed to the different type of coordination of the two groups to the palladium atom (η^2 and η^1, respectively).

Table 6
Selected bond lengths (Å) and angles (°) for $[Pd\{[Ph{-}C{=}C{-}Ph)_2(\eta^5{-}C_5H_3){-}CH{=}N{-}CH_2{-}CH_2{-}OH]Fe(\eta^5{-}C_5H_5)\}Cl]$ (**10**) [a]

Bond lengths			
Pd–C(14)	2.085(4)	Pd–C(21)	2.085(4)
Pd–C(28)	2.522(5)	Pd–C(35)	1.987(5)
Pd–χ	1.9791(4)	Pd–Cl(1)	2.215(2)
Pd–N	2.128(4)	N–C(11)	1.227(5)
N–C(12)	1.439(6)	C(12)–C(13)	1.471(7)
C(13)–O	1.326(6)	C(10)–C(14)	1.452(6)
C(14)–C(21)	1.427(6)	C(21)–C(28)	1.470(6)
C(28)–C(35)	1.294(5)	Fe–C_{ring} [b]	1.99(3)
C–C_{ring} [b]	1.37(3)		
Bond angles			
N–Pd–Cl(1)	90.36(12)	N–Pd–C(28)	136.55(14)
N–Pd–C(35)	165.1(2)	N–Pd–C(21)	103.7(2)
N–Pd–C(14)	96.9(2)	C(14)–Pd–Cl(1)	153.36(2)
C(21)–Pd–Cl(1)	103.7(2)	C(35)–Pd–Cl(1)	96.9(2)

[a] Estimated S.D. values in parenthesis.

[b] Average value for the ferrocenyl moiety.

The complex contains a [5,9] bicyclic system, which arises from the fusion of the substituted pentagonal ring of the ferrocenyl moiety and a nine-membered palladacycle formed by the set of atoms: Pd, N, C(11), C(9), C(10), C(14), C(21), C(28) and C(35).

The > C=N– functional group is contained in the nine-membered metallacycle, thus confirming its *endo*-structure. The imine ligand has an *anti*-conformation (*E*-form) as reflected in the torsion angle: C(9)–C(11)–N–C(12): 174.1(2)°. The distance between the two metal atoms (4.263(3) Å) is clearly longer than that found in the five-membered cyclopalladated complexes **6** (3.5635(3) Å) and **8** (3.5020(3) Å), and consequently there is no direct interaction between Pd and Fe.

The average C–C bond length in the two pentagonal rings (1.37(2) Å) is similar to the values reported for other ferrocene derivatives [28]. The Fe–C(ring) bond distance ranges from 1.941(5) to 2.049(4) Å. The longest bond distance corresponds to the Fe–C(10) bond which is directly involved in the insertion process. The two pentagonal rings are parallel (tilt angle: 3.79°) and their relative orientation deviates by 22.97° from the ideal eclipsed conformation.

The phenyl substituents on the double bond C(14)–C(21) are *trans* to each other, and those of the C(28)–C(35) are *cis*. This arrangement of the four phenyl groups is consistent with the common distribution of substituents of η^3-butadienyl fragments in nine-membered metallacycles formed by bis(insertion) processes [47–52]. The X-ray crystal structure of **10** shows that the C(14)–C(21) bond of the butadienyl fragment is located below the plane defined by the atoms N, C(11) and opposite to the iron center and the C_5H_5 ring of the ferrocenyl moiety, and that the phenyl ring at the C(14) atom is oriented towards the unsubstituted pentagonal ring.

---

[4] For **6**: the least-squares equation of the plane defined by the set of atoms [C(1)–C(5)] is: $(-0.1264)XO + (0.9516)YO + (-0.2801)ZO = 1.8224$. The deviations from the mean plane are: C(1), − 0.0005; C(2), + 0.0019; C(3), − 0.0025; C(4), 0.0022; C(5): − 0.0010 Å. The least-squares equation of the plane defined by the set of atoms [C(6)–C(10)] is: $(-0.1103)\ XO + (0.9512)\ YO + (-0.2882)\ ZO = -1.5156$. The deviations from the mean plane are: C(6), − 0.0001; C(7), 0.0031; C(8), − 0.0048; C(9), 0.0047; and C(10), − 0.0028 Å. For **8**: the least-squares equation of the plane defined by the set of atoms [C(1)–C(5)] is: $(-0.7515)XO + (0.5794)YO + (0.3153)ZO = 5.1555$. The deviations from the mean plane are the followings: C(1), + 0.021; C(2), − 0.011; C(3), − 0.002; C(4), + 0.015; and C(5), − 0.020 Å. The least-squares equation of the plane defined by the set of atoms [C(6)–C(10)] is: $(-0.7161)\ XO + (0.6373)\ YO + (0.2847)\ ZO = 8.9222$. The deviations from the mean plane are: C(6), − 0.024; C(7), + 0.001; C(8), − 0.001; C(9), −0.001; and C(10), − 0.002 Å.

[5] The least-squares equation of the plane defined by the atoms: Cl(1), N, C(35) and the middle point (χ) of the segment defined by C(14) and C(21) is: $(-0.2417)XO + (0.7099)YO + (0.6616)ZO = 4.8195$.

Table 7
Summary of the electrochemical data: anodic (E_{pa}) and cathodic (E_{pc}) potentials (in mV) for compounds under study [a]

Compound	E_{pa}	E_{pc}
$[(\eta^5\text{-}C_5H_5)Fe\{(\eta^5\text{-}C_5H_4){-}CH{=}N{-}CH_2{-}CH_2{-}OH\}]$ (**1**)	98	30
$[Pd\{[(\eta^5\text{-}C_5H_4){-}CH{=}N{-}CH_2{-}CH_2{-}OH]Fe(\eta^5\text{-}C_5H_5)\}_2\text{-}Cl_2]$ (**3**)	304	230
$[Pd\{[(\eta^5\text{-}C_5H_3){-}CH{=}N{-}CH_2{-}CH_2{-}OH]Fe(\eta^5\text{-}C_5H_5)\}\text{-}(\mu\text{-}Cl)]_2$ (**4**)	57	−43
$[Pd\{[(\eta^5\text{-}C_5H_3){-}CH{=}N{-}CH_2{-}CH_2{-}OH]Fe(\eta^5\text{-}C_5H_5)\}\text{-}Cl(PPh_3)]$ (**6**)	108	8
$[Pd\{[(\eta^5\text{-}C_5H_3){-}CH{=}N{-}CH_2{-}CH_2{-}OH]Fe(\eta^5\text{-}C_5H_5)\}\text{-}Cl(CNCMe_3)]$ (**8**)	72	25
$[Pd\{[Et{-}C{=}C{-}Et)_2(\eta^5\text{-}C_5H_3){-}CH{=}N{-}CH_2{-}CH_2{-}OH]\text{-}Fe(\eta^5\text{-}C_5H_5)\}Cl]$ (**9**)	318	201
$[Pd\{[Ph{-}C{=}C{-}Ph)_2(\eta^5\text{-}C_5H_3){-}CH{=}N{-}CH_2{-}CH_2{-}OH]\text{-}Fe(\eta^5\text{-}C_5H_5)\}Cl]$ (**10**)	336	231
$[Pd\{[MeO_2CC{=}CCO_2Me)_2(\eta^5\text{-}C_5H_3){-}CH{=}N{-}CH_2{-}CH_2{-}OH]Fe(\eta^5\text{-}C_5H_5)\}Cl]$ (**11**)	375	[b]

[a] The values given below refer to the ferrocene|ferricinium couple.
[b] No reduction peak was observed in the reverse scan.

2.5. Electrochemistry

Electrochemical studies based on cyclic voltammetry for compounds **1**, **3**–**11** were undertaken. In all cases the experiments were performed at ca. 20°C using 10^{-3} M solutions of the complexes in acetonitrile (HPLC grade) and using different scan rates (from 0.1 to 100 V s^{-1}).

The cyclic voltammogram of the ligand showed one anodic peak with a directly associated reduction peak in the reverse scan, which is attributed to the one-electron oxidation–reduction process (Table 7). The position of the peaks for **1** are consistent with the values reported for related ferrocenyl Schiff bases of general formula $[(\eta^5\text{-}C_5H_4){-}CH{=}N{-}R\}Fe(\eta^5\text{-}C_5H_5)]$ [23].

The cyclic voltammogram of **3** was similar to that of the free ligand except for the position of the wave which appeared strongly shifted to more anodic potentials ($E_{1/2} = 267$ mV). This is consistent with the results reported for $[(\eta^5\text{-}C_5H_5)Fe\{(\eta^5\text{-}C_5H_4){-}CH{=}N{-}NMe_2\}]$ ($E_{1/2} = -30$ mV) and *trans*-$[Pd\{(\eta^5\text{-}C_5H_5)Fe\{(\eta^5\text{-}C_5H_4){-}CH{=}N{-}NMe_2\}Cl_2]$ [39] ($E_{1/2} = 320$ mV), thus suggesting that the coordination of the palladium to the N-donor ligands inhibits the oxidation of the ferrocenyl unit. Except for compound **11**, the cyclic voltammograms of the remaining palladium(II) compounds also showed one anodic peak with a directly associated reduction peak in the reverse scan. The tendency of the ferrocenyl unit to oxidize in the palladium(II) complexes containing five-membered rings and a $\sigma(Pd{-}C_{sp^2,ferrocene})$ bond depends on the nature of the remaining ligands bound to the palladium, as reflected in the increase of the E_{pa} values which follow the sequence **4** < **8** < **6**. These findings are consistent with data reported for related cyclopalladated complexes derived from N-donor ferrocenyl units for which the di-μ-chloro derivatives were less resistant to oxidation than their analogues of general formula $[Pd(C^\wedge N)\text{-}Cl(PR_3)]$ [14,23,41]. For compounds **9**–**11** the oxidation occurs at higher potentials, thus indicating that the nine-membered cyclopalladated complexes are more resistant to oxidation than the free ligand **1** and the five-membered palladacycles **4**, **6** and **8**. For complex **11**, no reduction peak was detected in the reverse scan, thus suggesting that the oxidation is electrochemically irreversible.

2.6. Conclusions

The results presented in this study, show the great versatility of the coordination mode of the ferrocenyl Schiff base **1**. In compounds **2** and **3** it binds to the M(II) ion through the imine nitrogen exclusively, thus acting as a neutral N-donor group, while in the cyclopalladated derivatives **4**–**8** the ferrocenyl imine behaves as monoanionic $(C,N)^-$ bidentate ligand. The studies of the reactivity of the '$Pd(\mu\text{-}Cl)_2Pd$' moiety and of the $\sigma(Pd{-}C_{sp^2,ferrocene})$ bond allowed the isolation and characterization of monomeric complexes containing five- (for **5**–**8**) or nine-membered palladacycles (**9**–**11**). As well as this, the $\sigma(Pd{-}C_{sp^2,ferrocene})$ bond (in **4**) exhibits greater tendency to undergo the bis(insertion) of the alkynes $R{-}C{\equiv}C{-}R$ than the $\sigma(Pd{-}C_{sp^2,aryl})$ bond in $[Pd\{R{-}C_6H_3{-}CH{=}N{-}C_6H_4\text{-}4\text{-}CH_3\}(\mu\text{-}CH_3COO)]_2$ (**I**) (with R = 5-NO_2 (**Ib**), 4-NO_2 (**Ic**), 5-Cl (**Id**) or 4-Cl (**Ie**)). However, attempts to insert *tert*-butylisonitrile into the $\sigma(Pd{-}C_{sp^2,ferrocene})$ bond of **4** were unsuccessful in all the studied cases. This observation differs from the results obtained for $[Pd\{5'\text{-}OCH_3{-}C_6H_3{-}CH{=}N{-}C_6H_4\text{-}4\text{-}CH_3\}(\mu\text{-}Cl)]_2$ (**Ia**), which contains a $\sigma(Pd{-}C_{sp^2,aryl})$ bond, which reacted with the same isonitrile under identical experimental conditions.

3. Experimental

3.1. General comments

Ferrocenecarboxaldehyde, 2-ethanolamine, triphenylphosphine, deuterated pyridine, 1,2-bis(diphenylphosphino)ethane and the alkynes: hex-3-yne, diphenylacetylene and dimethylacetylenedicarboxylate were obtained from standard sources and used as received. *cis*-$[PtCl_2(dmso)_2]$ was prepared as described before [53]. Some of the preparations described below require benzene, which should be handled with **CAUTION**.

Elemental analyses (C, H, N and S (for **3**)) were carried out at the Serveis Científico-Tècnics (U.B.).

Infrared spectra were obtained with a Nicolet Impact-400 FTIR instrument using KBr pellets. Routine ^{1}H-NMR spectra were recorded at ca. 20°C on a Gemini 200 MHz instrument using $CDCl_3$ (99.5%) as solvent and $SiMe_4$ as internal standard. $^{13}C\{^1H\}$-NMR spectra were preformed ca. 20°C with a Varian 300 NMR instrument using $CDCl_3$ as solvent and $SiMe_4$ as internal standard. The spectra $^1H-^{13}C$ two-dimensional NMR were run at 500 MHz either using a Varian VXR-500 or a Bruker Avance DMX 500 instrument. Heteronuclear single-quantum coherence $^1H-^{13}C$ (HSQC) with gradient selection and phase-sensitive experiments were recorded. A total of 2 × 128 increments of 2 K spectra (two scans) were collected and zero-filled to 512 in F_1 and 4096 in F_2.

$^{31}P\{^1H\}$-NMR spectra of compounds **6** and **7** were recorded at ca. 20°C with a Bruker 250 DXR instrument using $CDCl_3$ as solvent and $P(OMe)_3$ as standard, (δ ^{31}P [$P(OMe)_3$]=140.17 ppm). $^{195}Pt\{^1H\}$-NMR spectrum of **2** was recorded with a Bruker 250 DXR instrument using $CDCl_3$ as solvent.

3.2. Preparation of the compounds

*3.2.1. [{(η^5-C_5H_4)–CH=N–CH_2–CH_2–OH}]Fe-(η^5-C_5H_5)] (**1**)*

Ferrocenecarboxaldehyde (1.090 g, 5.1×10^{-3} mol) was suspended in 20 cm^3 of benzene and stirred at room temperature for 10 min. The undissolved materials were filtered out and discarded. Then, 0.311 g (5.1×10^{-3} mol) of 2-aminoethanol was added to the filtrate. The reaction flask was connected to a condenser equipped with a Dean–Stark apparatus. The mixture was refluxed in an ethyleneglycol bath until ca. 10 cm^3 had condensed in the Dean–Stark apparatus. Then, the hot solution was carefully filtered out, and the filtrate was allowed to cool to room temperature. During this period, bright-orange needles formed. The crystals were collected by filtration and air-dried. (Yield: 82%). Characterization data: Anal. Calc. for $C_{13}H_{15}NOFe$: C, 60.73; H, 5.88 and N, 5.45. Found: C, 60.5; H, 5.8; N, 5.6%. IR: ν(> C=N–): 1649 cm^{-1}.

*3.2.2. trans-[Pt{[(η^5-C_5H_4)=N–CH_2–CH_2–OH]-Fe(η^5-C_5H_5)}Cl_2(dmso)] (**2**)*

A 100 mg amount (2.37×10^{-4} mol) of *cis*-[$PtCl_2(dmso)_2$] was suspended in 20 cm^3 of methanol and refluxed until complete dissolved. Then a solution formed from 61 mg (2.37×10^{-4} mol) of **1** and 5 cm^3 of methanol was added, and the reaction mixture was stirred at room temperature for 5 h. The undissolved materials were removed by filtration and discarded. The red filtrate was then concentrated to ca. 10 cm^3 on a rotary evaporator. The deep-red solid formed was collected by filtration and air-dried (Yield: 45%). Characterization data: Anal. Calc. for $C_{15}H_{21}NO_2Cl_2FePtS$: C, 29.97; H, 3.52, N, 2.33 and S, 5.20. Found: C, 29.6; H, 3.5; N, 2.40; S, 5.3. IR: ν(> C=N–): 1629 cm^{-1}. ^{195}Pt-NMR (in ppm): −3025.

*3.2.3. trans-[Pd{[(η^5-C_5H_4)–CH=N–CH_2–CH_2–OH]-Fe(η^5-C_5H_5)}$_2Cl_2$] (**3**)*

A 200 mg (7.78×10^{-4} mol) amount of ligand **1** was dissolved in 5 cm^3 of methanol. Then a solution containing 114 mg (7.78×10^{-4} mol) of $Na_2[PdCl_4]$ and 5 cm^3 of methanol was added. The resulting mixture was stirred at room temperature (ca. 20°C) for 1 h. The orange–red solid formed during this period was collected by filtration, washed with methanol (ca. 3 cm^3) and air-dried. (Yield: 79%). Characterization data: Anal. Calc. for $C_{26}H_{30}N_2O_2Cl_2Fe_2Pd \cdot H_2O$: C, 44.01; H, 4.55; N, 3.95. Found: C, 43.8; H, 4.45; N, 3.9%. IR: ν(> C=N–): 1586 cm^{-1}.

*3.2.4. [Pd{[(η^5-C_5H_3)–CH=N–CH_2–CH_2–OH]-Fe(η^5-C_5H_5)}(μ-Cl)]$_2$ (**4**)*

A mixture containing the ferrocenylimine **1** (300 mg, 1.17×10^{-3} mol), $Na_2[PdCl_4]$ (0.344 g, 1.17 mmol), $Na(CH_3COO) \cdot 3H_2O$ (0.159 g, 1.17×10^{-3} mol) and 30 cm^3 of methanol was stirred at room temperature for 12 h. The solid formed was collected by filtration, washed with methanol (3 × 5 cm^3) and air-dried. (Yield: 59%). Compound **4** was recrystallized in CH_2Cl_2. Characterization data: Anal. Calc. for $C_{26}H_{28}N_2O_2Fe_2$-$Pd_2Cl_2CH_2Cl_2$: C, 36.82; H, 3.43; N, 3.19. Found: C, 36.9; H, 3.3; N, 3.2%. IR: ν(> C=N–): 1586 cm^{-1}.

*3.2.5. [Pd{[(η^5-C_5H_3)CH=N–CH_2–CH_2–OH]-Fe(η^5-C_5H_5)}Cl(py-d_5)] (**5**)*

This complex was prepared in situ and characterized by NMR spectroscopies. The method used for its synthesis was as follows: compound **4** (50 mg, 5.68×10^{-5} mol) was suspended in 0.7 cm^3 of $CHCl_3$, then an excess of deuterated pyridine (py-d_5) (10 μl, 1.2×10^{-4} mol) was added. The reaction mixture was shaken vigorously at room temperature (ca. 20°C) for 2 min to favor the dissolution of the di-μ-chloro cyclopalladated complex, and produced an orange solution.

*3.2.6. [Pd{[(η^5-C_5H_3)CH=N–CH_2–CH_2–OH]-Fe(η^5-C_5H_5)}Cl(PPh_3)] (**6**)*

Triphenylphosphine (115 mg, 4.4×10^{-4} mol) was added to a suspension containing 150 mg (2.2×10^{-4} mol) of **4** and 10 cm^3 of benzene. Then the reaction mixture was stirred at room temperature (ca. 20°C) for 1 h. The undissolved materials were removed by filtration and discarded. The filtrate was then concentrated to dryness on a rotary evaporator giving an orange–red residue, which was treated with the minimum amount of CH_2Cl_2. Addition of *n*-hexane produced the precipitation of a reddish solid which was collected by filtration and air-dried. (Yield: 75%). Characterization data: Anal. Calc. for $C_{31}H_{29}NOFePPdCl$: C, 56.3; H, 4.43; N, 2.12. Found: C, 56.25; H, 4.45; N, 2.0%. IR: $\nu(>C{=}N-)$: 1602 cm^{-1}. ^{31}P-NMR (in ppm): 37.40.

3.2.7. *[Pd{[(η^5-C_5H_3)–CH=N–CH_2–CH_2–OH]-Fe(η^5-C_5H_5)}(dppe)]Cl (7)*

A 200 mg (2.9×10^{-4} mol) amount of **4** was suspended in 20 cm^3 of CH_2Cl_2. Then, a stoichiometric amount of dppe (225 mg, 5.8×10^{-4} mol) was added. The resulting mixture was stirred at room temperature (ca. 20°C) for 20 min and filtered out. The orange–red filtrate was concentrated to ca. 5 cm^3 on a rotary evaporator. Evaporation of the solvent at room temperature produced a microcrystalline red solid, which was collected by filtration and air-dried. (Yield: 71%). Characterization data: Anal. Calc. for $C_{38}H_{38}ClNOFeP_2$-Pd·1/2CH_2Cl_2: C, 55.93; H, 4.75; N, 1.67. Found: C, 55.6; H, 4.8; N, 1.7%. IR: $\nu(>C{=}N-)$: 1605 cm^{-1}. ^{31}P-NMR (in ppm): 48.04 and 62.38.

3.2.8. *[Pd{[(η^5-C_5H_3)=N–CH_2–CH_2–OH]-Fe(η^5-C_5H_5)}Cl(CNCMe$_3$)] (**8**)*

A 200 mg (2.9×10^{-4} mol) amount of **4** was suspended in 20 cm^3 of CH_2Cl_2. Then, the stoichiometric *tert*-butylisonitrile (70 μl, 6.1×10^{-4} mol) was added. The resulting mixture was stirred at room temperature (ca. 20°C) for 2 h and filtered out. The red filtrate was concentrated to ca. 5 cm^3 on a rotary evaporator. Evaporation of the solvent at room temperature produced small red–violet crystals, which were collected by filtration and air-dried. (Yield: 65%). Characterization data: Anal. Calc. for $C_{18}H_{23}ClN_2OFePd$: C, 44.94; H, 4.82; N, 5.82. Found: C, 45.0; H, 4.9; N, 5.75%. IR: $\nu(>C{=}N-)$: 1605 cm^{-1}.

3.2.9. *[Pd{[(R–C=C–R)$_2$(η^5-C_5H_3)–CH=N–CH_2–CH_2–OH]Fe(η^5-C_5H_5)}Cl] (R = Et (**9**), Ph (**10**) or CO_2Me (**11**))*

Complex **4** (206 mg, 3.0×10^{-4} mol) was suspended in 20 cm^3 of $CHCl_3$, then 1.2×10^{-3} mol of the corresponding alkyne was added dropwise for ca. 10 min. Once the addition had finished, the reaction mixture was refluxed for 1.5 h. The resulting red–brown solution was filtered out and the filtrate was concentrated to ca. 5 cm^3 on a rotary evaporator. The residue was then passed through a SiO_2 column (10 mm × 250 mm). Elution with a 100:1 $CHCl_3$–CH_3OH mixture released an orange band, which was concentrated to dryness on a rotary evaporator giving an orange solid, which was collected and vacuum dried. (Yields: 67, 62 and 56% for **9**, **10** and **11**, respectively). Good crystals for X-ray analyses of **10** were obtained by slow evaporation of a CH_2Cl_2 solution at room temperature. Characterization data for **9**: Anal. Calc. for $C_{25}H_{34}ClNOFePd$: C, 53.41; H, 6.10; N, 2.49. Found: C, 53.7; H, 6.2; N, 2.3%. IR: $\nu(>C{=}N-)$: 1628 cm^{-1}. For **10**: Anal. Calc. for $C_{41}H_{34}ClNOFePd\cdot CH_2Cl_2$: C, 60.10; H, 4.32; N, 1.67. Found: C, 60.05; H, 4.4; N, 1.7%. IR: $\nu(>C{=}N-)$: 1632 cm^{-1}. For **11**: Anal. Calc. for $C_{25}H_{26}ClNO_9FePd$: C, 44.02; H, 3.84; N, 2.05. Found: C, 43.95; H, 3.85; N, 1.9%. IR: $\nu(>C{=}N-)$: 1640 cm^{-1}.

3.3. *Electrochemistry*

Cyclic voltammograms were obtained on a VERSSTAT potentiostat under argon at 25°C using acetonitrile as solvent and [Bu_4N][PF_6] (0.1 mol × dm^{-3}) as supporting electrolyte. The potentials were referred to an Ag|$AgNO_3$ (0.1 mol × dm^{-3}) electrode separated from the solution by a medium-porosity fritted disc. A platinum wire auxiliary electrode was used in conjunction with a platinum disc working electrode and a Tacussel EDI-rotary electrode (3.14 mm^2). A cyclic voltammogram of freshly prepared (10^{-2} mol dm^{-3}) solution of the complexes in CH_3CN was recorded at 10 V s^{-1}, and the values of the measured potentials were afterwards referred to the ferrocene|ferrocenium couple, which was used as internal reference.

3.4. *Crystal structure analyses of **1**, **6**, **8** and **10***

A prismatic crystal (0.1 × 0.1 × 0.2 mm) of **1**, **6**, **8** or **10** was selected and mounted on an Enraf–Nonius CAD4 four circle diffractometer. Unit cell parameters (Table 8) were determined from automatic centering of 25 reflections in the range $12<\theta<21°$ and refined by the least-squares method in all cases. Intensities were collected with a graphite monochromated Mo–K$_\alpha$ radiation, using a $\omega/2\theta$ scan technique. A total of 1913 reflections (for **1**), 6349 reflections (for **6**), 4625 reflections (for **8**) and 4389 (for **10**) were measured in the ranges: $2.44<\theta<29.5°$, $2.20<\theta<29.97°$, $2.44<\theta<29.97°$ and $2.20<\theta<31.51°$ for **1**, **6**, **8** and **10**, respectively. The number of non-equivalent reflections by symmetry was 1913 for **1** [R_{int} (on I) = 0.053], 6290 for **6** [R_{int} (on I) = 0.017], 4446 for **8** [R_{int} (on I) = 0.042] and 4389 for **10** [R_{int} (on I) = 0.014]. The number of observed reflections [$I>2\sigma(I)$] is given in Table 8. Three reflections were measured every 2 h as orientation and intensity control and no significant decay was observed. Lorentz polarization corrections were performed, but absorption corrections were not.

The structures were solved by direct methods using the SHELXS computer program [54] and refined by full-matrix least-squares methods with the SHELX-93 computer program [55] using 1846 reflections (for **1**), 6420 (for **6**), 4396 (for **8**) and 5952 (for **10**) (very negative intensities were not assumed). The functions minimized were: $\Sigma\, w\, \|F_o|^2-|F_c|^2|^2$, where $w=[\sigma^2(I)+$

Table 8
Crystal data and details of the refinement of the crystal structure of compounds: $[(\eta^5\text{-}C_5H_5)Fe\{(\eta^5\text{-}C_5H_4)\text{–}CH{=}N\text{–}CH_2\text{–}CH_2\text{–}OH\}]$ (**1**), $[Pd\{[(\eta^5\text{-}C_5H_3)\text{–}CH{=}N\text{–}CH_2\text{–}CH_2\text{–}OH]Fe(\eta^5\text{-}C_5H_5)\}Cl(PPh_3)]$ (**6**), $[Pd\{[(\eta^5\text{-}C_5H_3)\text{–}CH{=}N\text{–}CH_2\text{–}CH_2\text{–}OH]Fe(\eta^5\text{-}C_5H_5)\}Cl(CNCMe_3)]$ (**8**) and $[Pd\{[(Ph\text{–}C{=}C\text{–}Ph)_2(\eta^5\text{-}C_5H_3)\text{–}CH{=}N\text{–}CH_2\text{–}CH_2\text{–}OH]Fe(\eta^5\text{-}C_5H_5)\}Cl]$ (**10**)

	1	**6**	**8**	**10**
Empirical formula	$C_{13}H_{15}FeNO$	$C_{31}H_{29}ClFeNOPdP$	$C_{18}H_{23}ClFeN_2OPd$	$C_{42}H_{36}Cl_3FeNOPd$
Formula weight	257.11	660.22	481.08	839.32
T (K)	293(3)	293(2)	293(2)	293(2)
λ (Mo–K_α) (Å)	0.71069	0.71069	0.71069	0.71069
Crystal system	Monoclinic	Triclinic	Monoclinic	Triclinic
Space group	$P2_1/a$	$P\bar{1}$	$P2_1/c$	$P\bar{1}$
a (Å)	7.779(6)	9.838(9)	7.575(10)	10.165(7)
b (Å)	10.159(5)	11.016(5)	16.689(13)	12.304(6)
c (Å)	14.816(4)	13.660(3)	15.040(4)	14.960(10)
α (°)	90.0	96.60(3)	90.0	83.56(5)
β (°)	100.54(5)	96.06(4)	95.84(6)	78.51(5)
γ (°)	90.0	108.02(5)	90.0	67.65(4)
V (Å^3)	1151.1(11)	1382.8(14)	1892(3)	1694(2)
$D_{\text{calc.}}$ (mg m^{-3})	1.484	1.586	1.689	1.645
μ (mm^{-1})	1.286	1.354	1.865	1.232
$F(000)$	536	668	968	852
θ Range (°)	2.44, 29.95	2.20, 29.97	2.44, 29.97	2.20, 31.51
Index ranges	$-10 \leq h \leq 10$, $0 \leq k \leq 14$, $0 \leq l \leq 20$	$-13 \leq h \leq 13$, $-15 \leq k \leq 15$, $0 \leq l \leq 19$	$-10 \leq h \leq 10$, $0 \leq k \leq 23$, $0 \leq l \leq 21$	$-14 \leq h \leq 14$, $-16 \leq k \leq 17$, $0 \leq l \leq 20$
No. of reflections collected	1913	6349	4625	6019
No. of independent reflections	1846	6290	4446	5952
[R_{int}(on F)]	0.0539	0.0172	0.0429	0.0144
Refinement method	Full-matrix least-squares on F^2			
No. of data	1846	6420	4396	5952
No. of parameters	202	450	199	503
Goodness of fit on F^2	0.814	1.035	1.037	0.786
Final R [$I > 2\sigma(I)$]	$R_1 = 0.0397$, $wR_2 = 0.0666$	$R_1 = 0.0485$, $wR_2 = 0.0998$	$R_1 = 0.0583$, $wR_2 = 0.1431$	$R_1 = 0.0389$, $wR_2 = 0.0631$
R indices (all data)	$R_1 = 0.0763$, $wR_2 = 0.0733$	$R_1 = 0.0586$, $wR_2 = 0.1088$	$R_1 = 0.0673$, $wR_2 = 0.1626$	$R_1 = 0.0692$, $wR_2 = 0.0687$
Largest difference peak and hole (e Å^{-3})	0.413 and −0.438	0.429 and −0.471	0.460 and −0.170	0.700 and −0.611

$(0.00186P)^2]^{-1}$ for **1**; $w = [\sigma^2(I) + (0.0513P)^2]^{-1}$ for **6**, $w = [\sigma^2(I) + (0.1021P)^2]^{-1}$ for **8**, and $w = [\sigma^2(I) + (0.0105P)^2]^{-1}$ for **10**, and $P = [|F_o|^2 + 2|F_c|^2]/3$. f, f' and f'' were taken from the literature [56]. For **1**, 14 hydrogen atoms were located from a difference synthesis and refined with an overall isotropic temperature factor and one hydrogen was computed and refined with an overall isotropic temperature factor using a riding model. For compounds **6** and **8**, all hydrogen atoms were located from a difference synthesis and refined with an overall isotropic temperature factor. For **10**, 15 hydrogen atoms were located from a difference syntheses and were refined with an overall isotropic temperature factor, and 21 hydrogen atoms were computed and refined with an overall isotropic temperature factor using a riding model. The final R (on F) factors were 0.039, 0.048, 0.058 and 0.038 for **1**, **6**, **8** and **10**, respectively, and wR (on $|F|^2$) = 0.066 (for **1**), 0.099 (for **6**), 0.143 (for **8**) and 0.063 (for **10**). Further details concerning the refinement of the structures of compounds **1**, **6**, **8** and **10** are summarized in Table 8.

4. Supplementary material

Further details of the crystal structures (CIF files) of compounds **1**, **6**, **8** and **10** are available from the Cambridge Crystallographic Data Centre. CCDC nos.: 127947 (for **1**), 127948 (for **6**), 127949 (for **8**) and 127950 (for **10**). Copies of this information may be obtained free of charge from: The Director, CCDC, 12 Union Road, Cambridge, CB2 1EZ, UK (fax: +44-1223-336033; email: deposit@ccdc.cam.ac.uk or www: http://www.ccdc.cam.ac.uk).

Acknowledgements

We thank the Ministerio de Educación and the Generalitat de Catalunya for financial support (Grants: PB96-0164 and 1997-SRG-0044). We are also grateful to Dr C. Muller (Departament de Química-Física, U.B.) for the facilities provided for the electrochemical studies.

References

[1] A. Togni, Ferrocenes. Homogeneous Catalysis. Organic Synthesis. Materials Sciences, VCH, Weinheim, 1995.
[2] W.R. Cullen, J.D. Woolins, Coord. Chem. Rev. 39 (1981) 1.
[3] I.R. Whittall, A.M. McDonagh, M.G. Humphrey, M. Samoc, in: F.G.A. Stone, R. West (Eds.), Advances in Organometallic Chemistry, vol. 42, Academic Press, San Diego, CA, 1998, p. 291.
[4] O. Crespo, M.C. Gimeno, P.G. Jones, A. Laguna, C. Sarroca, Chem. Commun. (1998) 1481.
[5] J.M. Poblet, M. Bénard, Chem. Commun. (1998) 1179.
[6] K. Severin, R. Bergs, W. Beck, Angew. Chem. Int. Ed. Engl. 37 (1998) 1634.
[7] Y. Nishibayashi, I. Takei, S. Uemura, M. Hidai, Organometallics 17 (1998) 3420.
[8] L. Schwink, P. Knochel, T. Eberle, J. Okuda, Organometallics 17 (1998) 7.
[9] S. Back, H. Pritzkow, H. Lang, Organometallics 17 (1998) 41.
[10] W.C. du Plessis, T.G. Vosloo, J.C. Swarts, J. Chem. Soc. Dalton Trans. (1998) 2507.
[11] M.A. Zhuravel, D.S. Glueck, L.M. Liable-Sands, A.L. Rheingold, Organometallics 17 (1998) 574.
[12] C. Jiang, Y.S. Wen, L.K. Liu, T.S.A. Hor, Y.K. Yan, Organometallics 17 (1998) 173.
[13] A.D. Ryabov, G.M. Kazankov, I.M. Payashkina, O.V. Grozovsky, O.G. Dyachenko, V.A. Polyakov, L.G. Kuz'mina, J. Chem. Soc. Dalton Trans. (1997) 4385.
[14] C. López, R. Bosque, X. Solans, M. Font-Bardía, New J. Chem. 22 (1998) 977.
[15] C.E.L. Headford, R. Mason, P.R. Ranantunge-Bandarage, B.H. Robinson, J. Simpson, J. Chem. Soc. Chem. Commun. (1990) 601.
[16] R. Costa, C. López, E. Molins, E. Espinosa, Inorg. Chem. 37 (1998) 5686.
[17] A. Benito, J. Cano, R. Martinez-Máñez, J. Soto, J. Payá, F. Lloret, M. Julve, J. Faus, M.D. Marcos, Inorg. Chem. 32 (1993) 1197.
[18] M. Bracci, C. Ercolani, B. Floris, M. Bassetti, A. Chiesi-Villa, C. Guastini, J. Chem. Soc. Dalton. Trans. (1990) 1357.
[19] A. Louati, M. Gross, L. Douce, D. Matt, J. Organomet. Chem. 438 (1992) 167.
[20] K. Hamamura, M. Kita, M. Nonoyama, J. Fujita, J. Organomet. Chem. 463 (1993) 169.
[21] C. López, R. Bosque, X. Solans, M. Font-Bardía, J. Silver, G. Fern, J. Chem. Soc. Dalton Trans. (1995) 1839.
[22] J.C. Kotz, E.E. Getty, L. Lin, Organometallics 4 (1985) 610.
[23] R. Bosque, C. López, J. Sales, Inorg. Chim. Acta 244 (1996) 141.
[24] C. López, J. Sales, X. Solans, R. Zquiak, J. Chem. Soc. Dalton Trans. (1992) 2321.
[25] R. Bosque, C. López, J. Sales, X. Solans, M. Font-Bardía, J. Chem. Soc. Dalton Trans. (1994) 735.
[26] R. Bosque, M. Font-Bardía, C. López, J. Sales, J. Silver, X. Solans, J. Chem. Soc. Dalton Trans. (1994) 747.
[27] C. López, R. Bosque, X. Solans, M Font-Bardia, New. J. Chem. 20 (1996) 1285.
[28] T.H. Allen, O. Kennard, Chem. Des. Automat. News 8 (1993) 146.
[29] Y.J. Wu, L. Ding, H.X. Wang, Y.H. Liu, H.Z. Yuan, X.A. Mao, J. Organomet. Chem. 535 (1997) 49.
[30] R. Bosque, C. López, X. Solans, M. Font-Bardía, Organometallics 18 (1999) 1267 and references therein.
[31] R. Bosque, C. López, J. Sales, X. Solans, J. Organomet. Chem. 483 (1994) 61.
[32] M. Pfeffer, Recl. Trav. Chim. Pays-Bas 109 (1990) 567.
[33] A.D. Ryabov, Synthesis (1985) 233.
[34] A. Albinati, P.S. Pregosin, R. Rüedi, Helv. Chim. Acta 68 (1985) 2046.
[35] C. Hansch, A. Leo, D. Hoekman, Exploring QSAR: Hydrophobic, Electronic and Steric Constants, ACS, Washington, DC, 1995.
[36] A.D. Ryabov, R. van Eldik, G. Le Borgne, M. Pfeffer, Organometallics 12 (1993) 1386.
[37] SPARTAN 5.0, Wavefunction Inc., 1995, 18401-Von Karman, Av. 370-Irvine, CA-92612, USA.
[38] G. Natile, F. Gasparrini, D. Misiti, G. Perego, J. Chem. Soc. Dalton Trans. 1977, 1747.
[39] C. López, R. Bosque, X. Solans, M. Font-Bardía, J. Organomet. Chem. 535 (1997) 99.
[40] C. López, J. Granell, J. Organomet. Chem. 555 (1998) 211.
[41] M. Benito, C. López, X. Solans, M. Font-Bardía, Tetrahedron: Asymm. 9 (1998) 4219.
[42] C. López, R. Bosque, D. Sainz, X. Solans, M. Font-Bardía, Organometallics 16 (1997) 3261.
[43] P.S. Pregosin, Coord. Chem. Rev. 44 (1982) 247.
[44] P.R.R. Ranatunge-Bandarage, N.W. Duffy, S.M. Johnston, B.H. Robinson, J. Simpson, Organometallics 13 (1994) 511.
[45] X. Riera, V. Moreno, M. Font-Bardía, X. Solans, Polyhedron 18 (1998) 65.
[46] A. Caubet, C. López, R. Bosque, J. Organomet. Chem. 577 (1999) 292.
[47] W. Tao, L.J. Silverberg, A.L. Rheingold, R.F. Heck, Organometallics 8 (1989) 2550.
[48] J.P. Sutter, M. Pfeffer, A. De Cian, J. Fischer, Organometallics 11 (1992) 386.
[49] M. Pfeffer, M.A. Rotteveel, J.P. Sutter, A. De Cian, J. Fischer, J. Organomet. Chem. 371 (1989) C21.
[50] M. Pfeffer, J.P. Sutter, A. De Cian, J. Fischer, Inorg. Chim. Acta 220 (1994) 115.
[51] C. López, X. Solans, D. Tramuns, J. Organomet. Chem. 471 (1994) 265.
[52] C. López, R. Bosque, X. Solans, M. Font-Bardía, J. Silver, G. Fern, J. Chem. Soc. Dalton Trans. (1995) 1839.
[53] J.H. Price, A.N. Williamson, R.F. Schramm, B.B. Wayland, Inorg. Chem. 11 (1972) 1280.
[54] G.M. Sheldrick, Acta Crystallogr. Sect. A 46 (1990) 467.
[55] G.M. Sheldrick, SHELXL-93, A Computer Program for Determination of Crystal Structures, University of Göttingen, Germany, 1994.
[56] International Tables of X-Ray Crystallography, vol. IV, Kynoch Press, Birmingham, UK, 1974, pp. 99, 100 and 149.